Molecular Therapy
Nucleic Acids
Original Article

Quantitative proteomics of the miR-301a/SOCS3/STAT3 axis reveals underlying autism and anxiety-like behavior

Xun Li,[1,2,5] Qi Fu,[1,5] Mingtian Zhong,[1,5] Yihao Long,[1] Fengyun Zhao,[1] Yanni Huang,[1] Zizhu Zhang,[3] Min Wen,[3] Kaizhao Chen,[1] Rongqing Chen,[4] and Xiaodong Ma[1]

[1]Key Laboratory of Brain, Cognition and Education Sciences, Ministry of Education, China; Institute for Brain Research and Rehabilitation, South China Normal University, Guangzhou 510631, China; [2]Hubei Key Laboratory of Tumor Microenvironment and Immunotherapy, College of Basic Medical Science, China Three Gorges University, Yichang 443002, China; [3]Guangdong Province Key Laboratory of Psychiatric Disorders, Department of Neurobiology, School of Basic Medical Sciences, Southern Medical University, Guangzhou 510515, China; [4]Guangdong Provincial Key Laboratory on Brain Function Repair and Regeneration, Department of Neurosurgery, Zhujiang Hospital, Southern Medical University, Guangzhou 510282, China

Autism is a widespread neurodevelopmental disorder. Although the research on autism spectrum disorders has been increasing in the past decade, there is still no specific answer to its mechanism of action and treatment. As a pro-inflammatory microRNA, miR-301a is abnormally expressed in various psychiatric diseases including autism. Here, we show that miR-301a deletion and inhibition exhibited two distinct abnormal behavioral phenotypes in mice. We observed that miR-301a deletion in mice impaired learning/memory, and enhanced anxiety. On the contrary, miR-301a inhibition effectively reduced the maternal immune activation (MIA)-induced autism-like behaviors in mice. We further demonstrated that miR-301a bound to the 3′UTR region of the SOCS3, and that inhibition of miR-301a led to the upregulation of SOCS3 in hippocampus. The last result in the reduction of the inflammatory response by inhibiting phosphorylation of AKT and STAT3, and the expression level of IL-17A in poly(I:C)-induced autism-like features in mice. The obtained data revealed the miR-301a as a critical participant in partial behavior phenotypes, which may exhibit a divergent role between gene knockout and knockdown. Our findings ascertain that miR-301a negatively regulates SOCS3 in MIA-induced autism in mice and could present a new therapeutic target for ameliorating the behavioral abnormalities of autism.

INTRODUCTION

The autism spectrum disorder (ASD) is a neurodevelopmental disorder that is mainly characterized by the deficit of social communication skills, restricted interests, and repetitive behaviors.[1] According to the latest data from the Food and Drug Administration, the incidence rate of children with autism has risen from 1 of 68 to 1 of 44 since 2010.[2] Maternal immune activation (MIA) during pregnancy has been recognized as an etiological risk factor for various psychiatric disorders.[3] Experiments in animal models suggested that MIA induced pro-inflammatory cytokines, which eventually altered the ASD behavioral phenotypes in the offspring.[4] Therefore, investigating the maternal immune system of autistic patients would highlight a novel therapeutic target for neuropsychiatric disorders.

The signal transducer and activator of transcription 3 (STAT3) is a major orchestrator of cellular immune processes, which regulate several cytokine and inflammatory immune mediators. The study of maternal immune pathogens has revealed the role of Stat3 activation in psychopathology within immune stimulation.[5] For example, microglial-specific STAT3 deletion reduced depressive-like behavior via neuronal synaptic activity.[6] Interestingly, the authors observed significant alleviation of communication deficits and repetitive stereotyped behaviors in BTBR T + tf/J (BTBR) autistic mice in the case of STAT3 inhibition.[7–9] Knocking down the raphe STAT3 expression in mice reduced the negative behavioral reactivity associated with psychopathology, indicating that serotonergic STAT3 acts as a molecular gate to tune behavioral reactivity.[10] Within multiple cells, STAT3 exerts a vital role in promoting cytokine production, such as interleukin (IL)-6 and IL-17A. IL-6 and IL-17A are key mediators for the abnormal cortical development and behavioral phenotypes in the MIA model. Injecting any of them into pregnant mice is sufficient to induce ASD-like behaviors in offspring.[11–13] Normally, IL-6 concentrations are maintained low during neurodevelopment of the fetal brain.[14] However, overexpression of IL-6 activates the JAK/STAT signaling pathway to promote the accumulation of

Received 5 December 2023; accepted 30 January 2024;
https://doi.org/10.1016/j.omtn.2024.102136.

[5]These authors contributed equally

Correspondence: Rongqing Chen, Guangdong Provincial Key Laboratory on Brain Function Repair and Regeneration, Department of Neurosurgery, Zhujiang Hospital, Southern Medical University, Guangzhou 510282, China.
E-mail: creatego@hptmail.com
Correspondence: Xiaodong Ma, Key Laboratory of Brain, Cognition and Education Sciences, Ministry of Education, China; Institute for Brain Research and Rehabilitation, South China Normal University, Guangzhou 510631, China.
E-mail: sciencema@hotmail.com

neuronal and glial cells with excessive inflammation, which leads to abnormal phenotypes in offspring. Recently, IL-17A has been identified as a critical mediator in autism and schizophrenia by reshaping diverse behavior phenotypes.[12,15]

Currently, several miRNAs have been implicated in neuropsychiatric disorders. For example, overexpression of miR-137 is thought to impair synaptic plasticity in hippocampal-dependent learning and memory.[16] A study on miR-124 has demonstrated that this particular microRNA attenuates depressive-like behavior by reducing microglial activation in hippocampus.[17] Furthermore, various studies implicated that miR-130 and miR-301 are related to ASD,[18] epilepsy,[19] depression, and cognitive impairment.[20] Here, our focus is on the study of the miR-301a and its dependent signaling pathways in autism-like behaviors for the following reasons: (1) aberrant expression of miR-301a has been identified in several neuropsychiatric disorders.[21] In the blood serum of autistic children, downregulation of the miR-301a has been detected.[22] (2) miR-130/301 was involved in neuropathology as it targets several high-risk ASD genes. Another study showed that overexpression of miR-130a reduced the length of neurites of cortical neurons and inhibited the dendritic spine formation by targeting MECP2.[23] PTEN and TSC1 are also well-known targets of miR-301a.[24,25] Moreover, experiments on mice demonstrated that deletion of PTEN or TSC1 produced autism-like behavioral deficits.[26,27] (3) miR-301a is a key positive regulator of inflammation by targeting STAT3 signaling pathways.[28] (4) miR-301a demonstrated a predominant function in both IL-6 and IL-17A in multiple genetic or epigenetic mice models.[29] These results indicated that miR-301a is involved in variety of neurological diseases. However, whether miR-301a is associated with autism or not remains unknown.

In the present study, we showed that deletion of miR-301a in mice led to abnormal behaviors, including social disability, increased anxiety, and cognitive impairment, but inhibition of miR-301a resulted in reduction of social novelty and depression levels in mice. We further demonstrated that SOCS3/STAT3 was targeted by miR-301a in hippocampus, which indicated SOCS3 as a new target of miR-301a. SOCS3 expression levels were significantly correlated with the age of ASD patients and implicated in MIA-induced offspring developing autism.[30] We hypothesize that SOCS3 upregulation sufficiently suppresses pro-inflammatory cytokines, such as IL-6 and IL-17A. Our findings illustrate the complex regulation of miR-301a in neuropsychiatric disorders and highlight miR-301a as a new target for the treatment of patients diagnosed with autism.

RESULTS

Study of abnormal behaviors in WT and *miR-301a*$^{-/-}$ mice

To explore the role of miR-301a in psychiatric disorders, we compared the expression of miR-130/301 family members in human tissues by using the online Tissue Atlas database. In the miR-130/301 family members, we found that miR-301a was the only miRNA with the highest expression in brain tissues (Figures S1A–S1D). Furthermore, we isolated several mouse tissues and measured the expression level of miR-301a by RT-PCR. Similar to human tissues, miR-301a was highly expressed in mouse brain tissues (Figure S1E). From the two public datasets, we also found that miR-301a was significantly downregulated in peripheral blood from adults with high-functioning ASDs compared with healthy controls[31]; however, there was no comparison of miR-301a expression in occipital and cerebellar tissues (Figures S2A–S2B).[32] These data implicated the critical role of miR-301a in maintaining local brain homeostasis.

Next, we performed a self-grooming and marble buried test to examine the repetitive behavior of mice. Our results showed that there was no significant difference in the repetitive behavior in wild-type (WT) mice and *miR-301a*$^{-/-}$ mice (Figures 1A and 1B). Second, we examined sociability and social novelty by using the three-chambered test. After habituation to the empty chambers, sociability test showed that both WT and *miR-301a*$^{-/-}$ mice displayed a significant preference for exploring the chamber with a stranger mouse over the empty chamber. However, WT but not *miR-301a*$^{-/-}$ mice exhibited a clear preference for the chamber with another stranger in the social novelty test, which suggested that WT mice had a better social novelty than *miR-301a*$^{-/-}$ mice (Figure 1C). In addition, we evaluated the recognition ability by the novel object recognition (NOR) test. We found that WT mice could distinguish the novel object, while *miR-301a*$^{-/-}$ mice could not identify it, suggesting that miR-301a deletion impaired the recognition ability (Figure 1D). Furthermore, *miR-301a*$^{-/-}$ mice showed fewer times of open arms and entries compared with WT mice by using elevated plus maze (EPM), suggesting that *miR-301a*$^{-/-}$ mice exhibited more anxiety, which is considered a stereotypical autistic-like behavior (Figure 1E).[33] These behavioral observations demonstrated that the deletion of miR-301a in mice reduced sociability, impaired learning/memory, and increased anxiety.

Quantitative proteomics analysis of WT and *miR-301a*$^{-/-}$ mouse brain tissues dissected from hippocampus, temporal cortex, and dorsal raphe nucleus

To investigate the molecular mechanism of behavioral impairment in miR-301a-deficient mice, we performed label-free quantitative mass spectrometry (MS) in hippocampus, temporal cortex, and dorsal raphe nucleus (DRN). We identified a total of 1,043 differential expressed proteins (541 were up- and 502 were downregulated) in hippocampus, 903 differential expressed proteins (463 were up- and 440 were downregulated) in temporal cortex, and 1,106 differential expressed proteins (562 were up- and 544 were downregulated) in DRN (Figures 2A and 2B; Table S1). Venn diagram showed 210 proteins were overlapping in these brain areas, and several of them were highly related to ASD such as Homer3, Syt1, Nrp1, Snap29, Ncam1, and Arf2 (Figure 2C).

Next, we analyzed the most enriched pathways based on the *Z* score to explore the underlined molecular by ingenuity pathway analysis (IPA).[34] The top 10 canonical pathways with the higher value of *Z* score in hippocampus, temporal cortex, and DRN are shown in Figure 2D. Eleven canonical pathways overlapped in these three areas, specifically the insulin signaling pathway and the super pathway of inositol phosphate compounds. They are highly correlated with ASD (Figures S3A–S3D). Though in DRN, we found that these

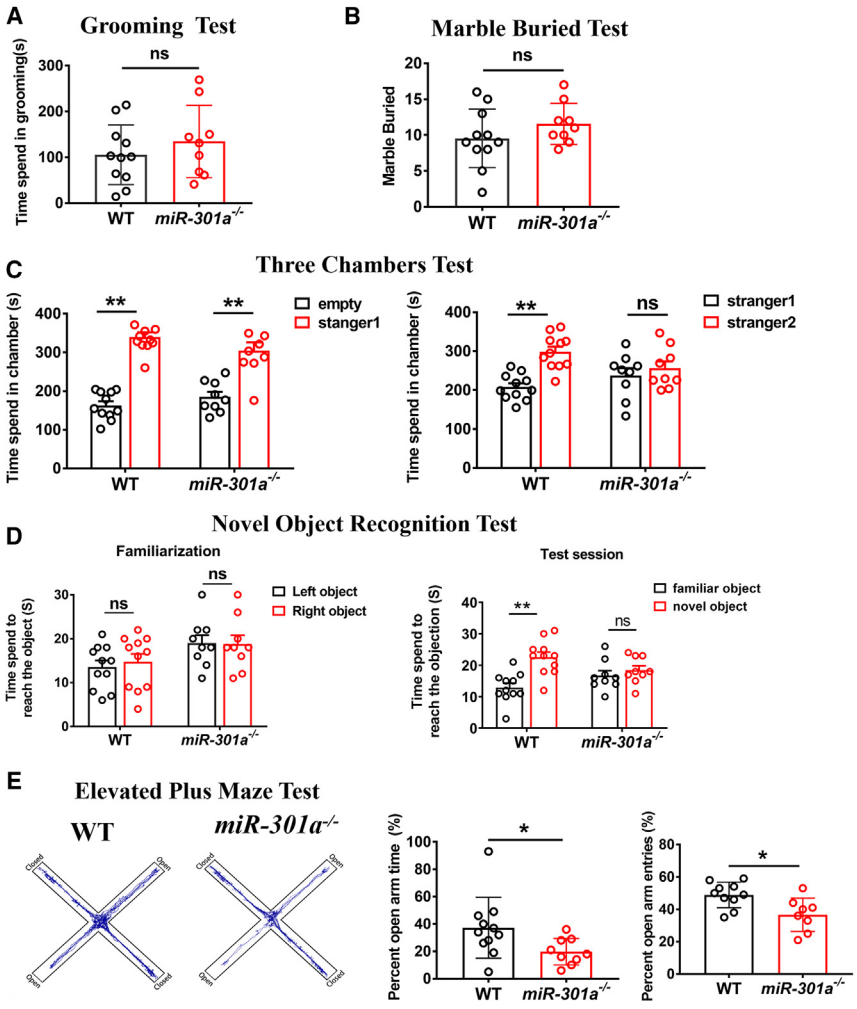

Figure 1. Autistic-like behaviors between WT and *miR-301a*$^{-/-}$ mice

(A) and (B) Both WT (n = 11) and *miR-301a*$^{-/-}$ (n = 9) mice showed no significant differences in time spent self-grooming (A) and buried marble (B). (C) Sociability assay was identified by the three-chamber test, and time spent in the chamber with either a mouse or an object was calculated. WT (n = 11) and *miR-301a*$^{-/-}$ (n = 9) mice. (D) In novel object recognition (NOR) test, WT mice (n = 11) had the ability to distinguish the novel object, but *miR-301a*$^{-/-}$ mice (n = 9) were not able to identify it. (E) In the elevated plus maze (EPM) test, representative track plots of the cumulative total distance of WT (n = 11) and *miR-301a*$^{-/-}$ (n = 9) mice. Percentage of total time spent in the open arms of the maze is presented. Each dot symbol represents an individual mouse. **p < 0.01 or *p < 0.05 indicates a significant difference between the indicated groups (two-tailed, unpaired Student's t test in A, B, and E, and two-way analysis of variance (ANOVA) in C and D). ns, not significant.

pathways were more enriched than in the other two brain areas. Moreover, several cytokine pathways such as IL-6, IL-3, IL-7, and granulocyte-macrophage colony-stimulating factor (GM-CSF) were enhanced in hippocampus, whereas multiple cholesterol-associated pathways were enriched in temporal cortex. Of note, we found the synaptogenesis signaling pathway was most enriched and present in hippocampus and DRN and it exhibited the highest activation signals in both areas.

Furthermore, we determined differences in the expression of several transcription factors, cytokines, kinases, and enzymes involved in the pathologic behavioral alterations in *miR-301a*$^{-/-}$ mice compared with WT. As shown in Figure 2E, we detected the highest levels of protein expression of transcription factors in hippocampus and DRN, but not in temporal cortex. The significant activation cytokines IL-4, tumor necrosis factor (TNF)-α, Oncostatin M (OSM), IL-6, and Prolactin (PRL) were associated with hippocampus (Table S2). Collectively, our results provided information on the underlying mechanisms and molecular targets in hippocampus, temporal cortex, and DRN in miR-301a-deficient mice.

MiR-301a deficiency induces large-scale changes of ASD-associated protein

Given that the deletion of miR-301a in mice led to abnormal behaviors, we sought to determine which miR-301a potential targets were involved in ASD. First, we analyzed the differentially expressed proteins related to ASD by using the online tool ToppGene Suite. The differentially expressed proteins in three brain regions were highly involved in psychiatric disorders, such as schizophrenia, epilepsy, Parkinson, ASD, seizures, and bipolar disorder (Figures S4A–S6A and Table S3). Next, we used the microRNA-target predicting database, which integrates Targetscan6.2, miRWalk2.0, miRDB4.0, miRanda-rel2010, RNA22V2, and PITA, to predict potential targets of miR-301a.[35] We chose those genes that were predicted by more than two databases to be as miR-301a potential targets and compared them with all upregulated proteins identified from those three brain areas (Figures S4B, S5B, and S6B), and identified 15, 10, and 11 significantly upregulated proteins in hippocampus, temporal cortex, and DRN, respectively (Figures S4C, S5C, and S6C). Correspondingly, these potential targets were implicated in constructed psychiatric networks including intellectual, anxiety, memory, cognitive, and behavior. For example, NCS1 and PED10A were associated with behavior, SCN1A with cognitive, and KDM5A with intellectual (Figures S4D, S5D, and S6D).

We chose three proteins (NCS1,[36] PDE10A,[16,37] and SCN1A[38,39]) that were highly related to autism-like behaviors and not reported as miR-301a targets, to further investigate whether the amounts of their mRNAs and proteins were affected by the miR-301a inhibitor. N2A cells were transfected with the anti-miR-301a inhibitor, and we detected a subsequently augmented expression of NCS1, PDE10A, and SCN1A

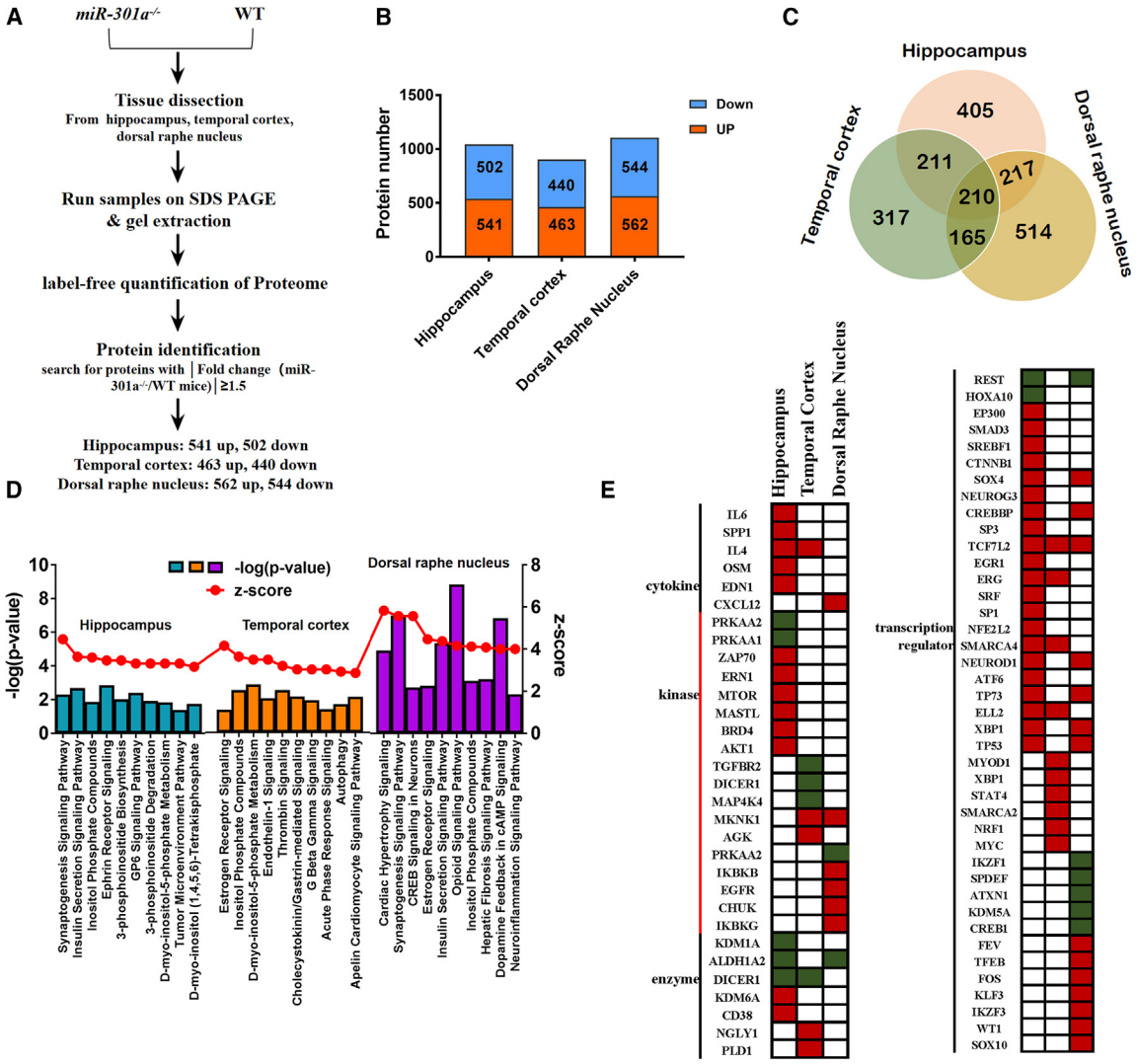

Figure 2. Quantitative proteomics analysis of hippocampus, temporal cortex and dorsal raphe nucleus between WT and *miR-301a*$^{-/-}$ mice

(A) Label-free quantitative mass spectrometry (MS) in the hippocampus, temporal cortex, and dorsal raphe nucleus. (B) Differentially expressed proteins identified in the hippocampus, temporal cortex, and dorsal raphe nucleus. (C) Venn diagram shown the intersecting of significant differentially expressed proteins in hippocampus, temporal cortex, and dorsal raphe nucleus. (D) The top 10 canonical pathways in hippocampus, temporal cortex, and dorsal raphe nucleus, respectively. (E) Upstream regulator analysis of the differentially expressed proteins in hippocampus, temporal cortex, and dorsal raphe nucleus (activation, red; inhibition, green; not significant, white).

proteins without changes in their mRNA expression level (Figures S7A and S7B). These results indicated that miR-301a may be highly involved in autism-like behaviors, and that the deletion of miR-301a suppressed the production of multiple targets at the translational level.

SOCS3 was identified as an miR-301a-direct target in the transcriptional signaling pathways

Given that most transcription factors and cytokines, especially IL-6, were highly activated in hippocampus, we next focused on this brain area to study the molecular mechanisms in both WT and *miR-301a*$^{-/-}$ mice. We performed RNA-sequencing using the total RNA isolated from hippocampus of the WT and *miR-301a*$^{-/-}$ mice and identified 73 differentially expressed genes (DEGs) (37 up- and 36 downregulated) (Figure 3A and Table S4). By analyzing biological processes, we found that IL-6 and JAK/STAT signaling pathways were enriched, which was similar to the above-presented proteomic results (Figure 3B). We then compared the DEGs with the data for the differentially expressed proteins from our proteomic analysis and found only four genes overlapped: SOCS3, TTR, IDE, and GM20521 (Figure 3C). SOCS3 is a negative regulator of the JAK/STAT3 signaling pathway.[40] Thus, we determined whether SOCS3 was a target gene of miR-301a in mouse hippocampus. The miRNA-target prediction analysis revealed the presence of one major binding site for miR-301a within SOCS3 RNA 3′UTR (Figure 3D). The luciferase reporter assay showed that miR-301a directly targeted 3′UTR of SOCS3 mRNA and downregulated its expression in 293T

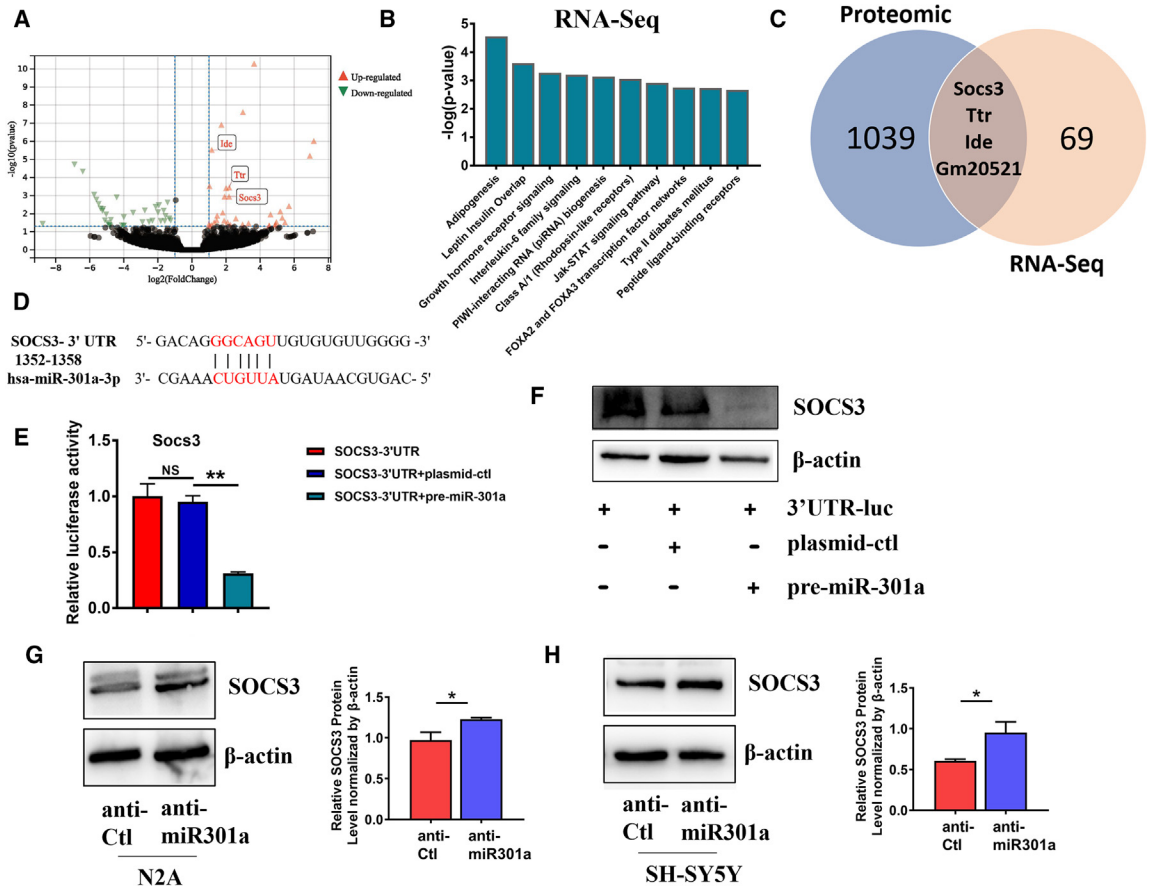

Figure 3. Identified miR-301a targets and signaling pathways involved in behavioral alterations in hippocampus

(A) Differentially regulated gene expression from RNA-sequencing (RNA-seq) analysis between WT and *miR-301a*$^{-/-}$ mice in the hippocampus. (B) In RNA-seq, the top 10 enriched biological processes of GO term between WT and *miR-301a*$^{-/-}$ mice. (C) Venn diagram of specific genes between differentially expressed proteins identified by proteomic analysis and DEGs identified by RNA-seq. (D) Prediction of major interference sites between miR-301a and the SOCS3 mRNA 3′UTR using TargetScan. (E) Luciferase activity in 293T cells transfected with the indicated luciferase reporter with either a control plasmid (plasmid-ctl) or a precursor miR-301a plasmid (pre-miR-301a). (F) Western blot analysis of SOCS3 expression in 293T cells with the indicated luciferase reporter with either plasmid-ctl or pre-miR-301a. (G and H) Western blot analysis of SOCS3 expression in N2A cells (G) and SH-SY5Y (H) transfected with either anti-Ctl or anti-miR-301a, and SOCS3 protein expression levels were quantified respectively. $^{**}p < 0.01$ or $^{*}p < 0.05$ indicates a significant difference between the indicated groups, unpaired Student's t test in G and H. ns, not significant.

cells (Figures 3E and 3F). In addition, SOCS3 expression was significantly upregulated in both N2A and SH-SY5Y cells transfected with anti-miR-301a compared with anti-control (Figures 3G and 3H). However, there was no significant upregulation of two high-risk genes for autism, PTEN, and TSC1 expression between the hippocampus tissues from WT mice and that from miR-301a KO mice (Figure S8A). These data suggested that miR-301a deletion affected the changes of protein levels by translation and that SOCS3 was a new identified miR-301a direct target that was possibly regulating the IL-6/STAT3, which is involved in ASD-like phenotype in mice.

miR-301a inhibition in WT mice ameliorated the anxiety-like behavior

The upregulation of SOCS3 has been reported to protect mice against neuroinflammatory responses in the CNS.[41] Therefore, in our experiments we further determined whether inhibiting miR-301a with a lock nucleic acid (LNA)-based oligonucleotide could effectively alter the impairment of behavior. For this purpose, we injected 20 mg/kg of miR-301a inhibitor into WT mice (anti-miR-301a). Compared with the control oligonucleotide (anti-Ctl), the anti-miR-301a mice significantly downregulated miR-301a expression in hippocampus of WT mice (Figure 4A). The open field test demonstrated that anti-miR-301a mice markedly reduced anxiety (Figure 4B), whereas exhibited no alteration on the repetitive stereotype (Figures 4C and 4D). Moreover, anti-miR-301a mice also significantly enhanced social interactions in the three-chamber social test (Figure 4E).

Next, we determined whether the miR-301a inhibition affected SOCS3 expression and STAT3 activation in hippocampus by western blot and immunofluorescence analyses. As shown in Figure 4F,

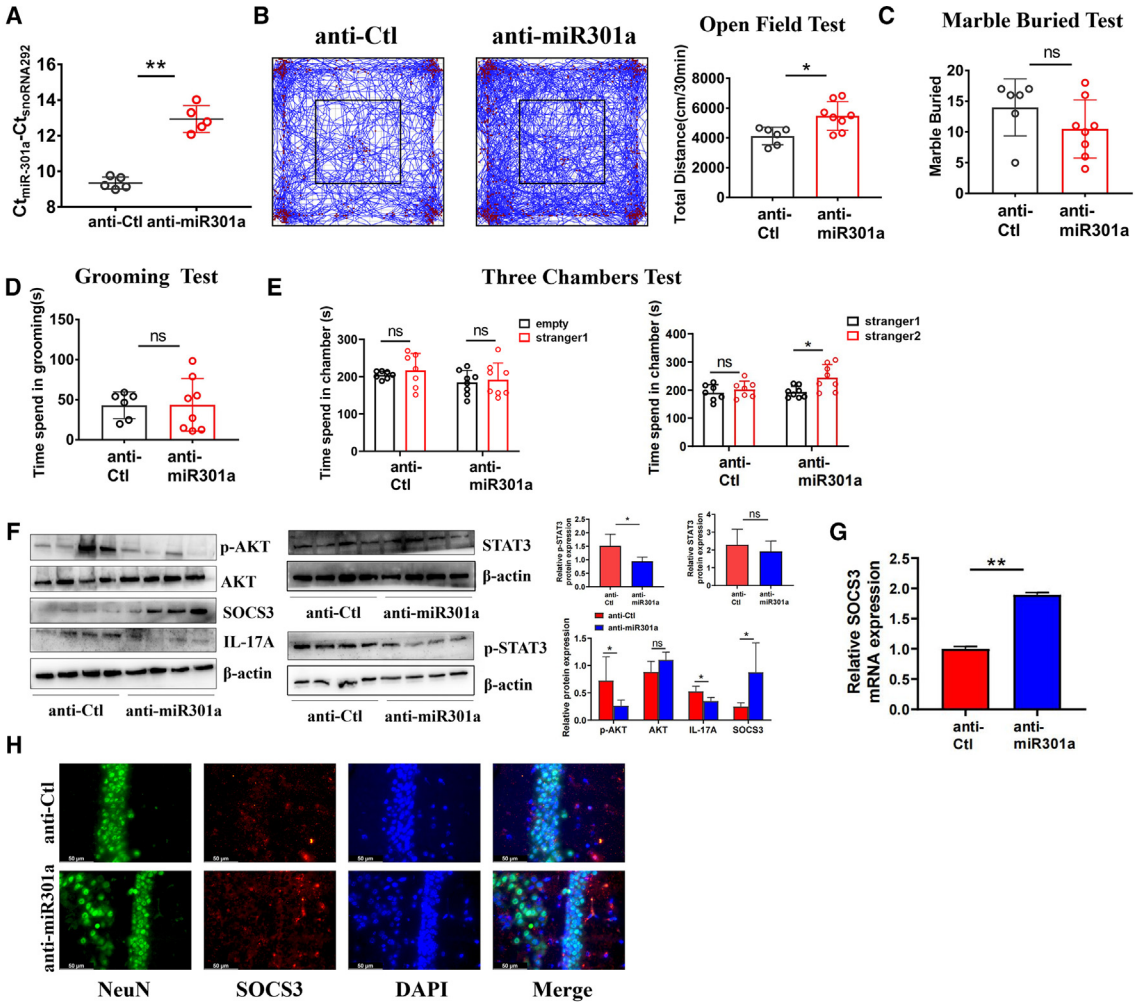

Figure 4. Reducing anxiety-like behavior in mice correlated with miR-301a knockdown *in vivo*

(A) The expression of miR-301a was evaluated by RT-PCR in hippocampus from WT mice injected with anti-Ctl or anti-miR-301a inhibitor via tail vein, respectively (n = 5 per group). (B) Mice with anti-miR-301a inhibitor administration displayed less frequency, duration, and distance moved in the center of the open field compared with mice with anti-Ctl (anti-Ctl) administration. Marble buried (C) and self-grooming (D) test showed no significant difference of repetitive behavior in mice between anti-Ctl injection (n = 6) and anti-miR301a injection (n = 8). (E) Sociability and novelty of WT mice injected with either anti-Ctl (n = 7) or anti-miR301a (n = 8) were identified by the three-chamber test and time spent in chamber with either a mouse or an object was calculated. (F) The activation of STAT3 and AKT, and the expression of SOCS3 and IL-17A were measured and quantified by western blot in hippocampus from adult mice with anti-Ctl (n = 4) and anti-miR301a administration (n = 4). (G) The mRNA expression of SOCS3 was measured by RT-PCR. (H) Immunofluorescence analysis of hippocampus tissues stained with NeuN (green) and SOCS3 (red) in mice with anti-Ctl (n = 4) and anti-miR301a administration (n = 4). DAPI (blue) was used for nucleus. Each dot symbol represents an individual mouse. $^{**}p < 0.01$ or $^{*}p < 0.05$ indicates a significant difference between the indicated groups (two-tailed, unpaired Student's t test in A, B, C, and D, and two-way analysis of variance [ANOVA] in E). ns, not significant.

SOCS3 expression was significantly upregulated, whereas the level of IL-17A, phosphorylated STAT3, and phosphorylated-AKT were downregulated in hippocampus from anti-miR-301a mice than anti-Ctl mice. The upregulation of SOCS3 was confirmed by RT-PCR and immunofluorescence analysis (Figures 4G, 4H, and S9A). Taken together, these results indicated that unlike the impairment of behaviors in miR-301a deficient mice, anti-miR-301a administration had protective roles for the anxiety and social interactions, which was associated with upregulation of SOCS3, thus reducing the activation of the AKT and STAT3 pathway.

miR-301a knockdown reversed the poly(I:C)-induced ASD-like behavior

The next question is whether miR-301a knockdown could ameliorate the ASDs in mice through NF-κB and STAT3, especially in the MIA-induced ASD mice model. Thus, we hypothesized that the inhibition of miR-301a could improve the behaviors in poly(I:C)-induced autistic mice models. We first injected poly(I:C) or saline into 12.5-day-old pregnant WT mice and collected the embryonic brain from mice treated with poly(I:C) or saline for 3 h and 7 days. Compared with the saline-treated controls, the expression of miR-301a remained

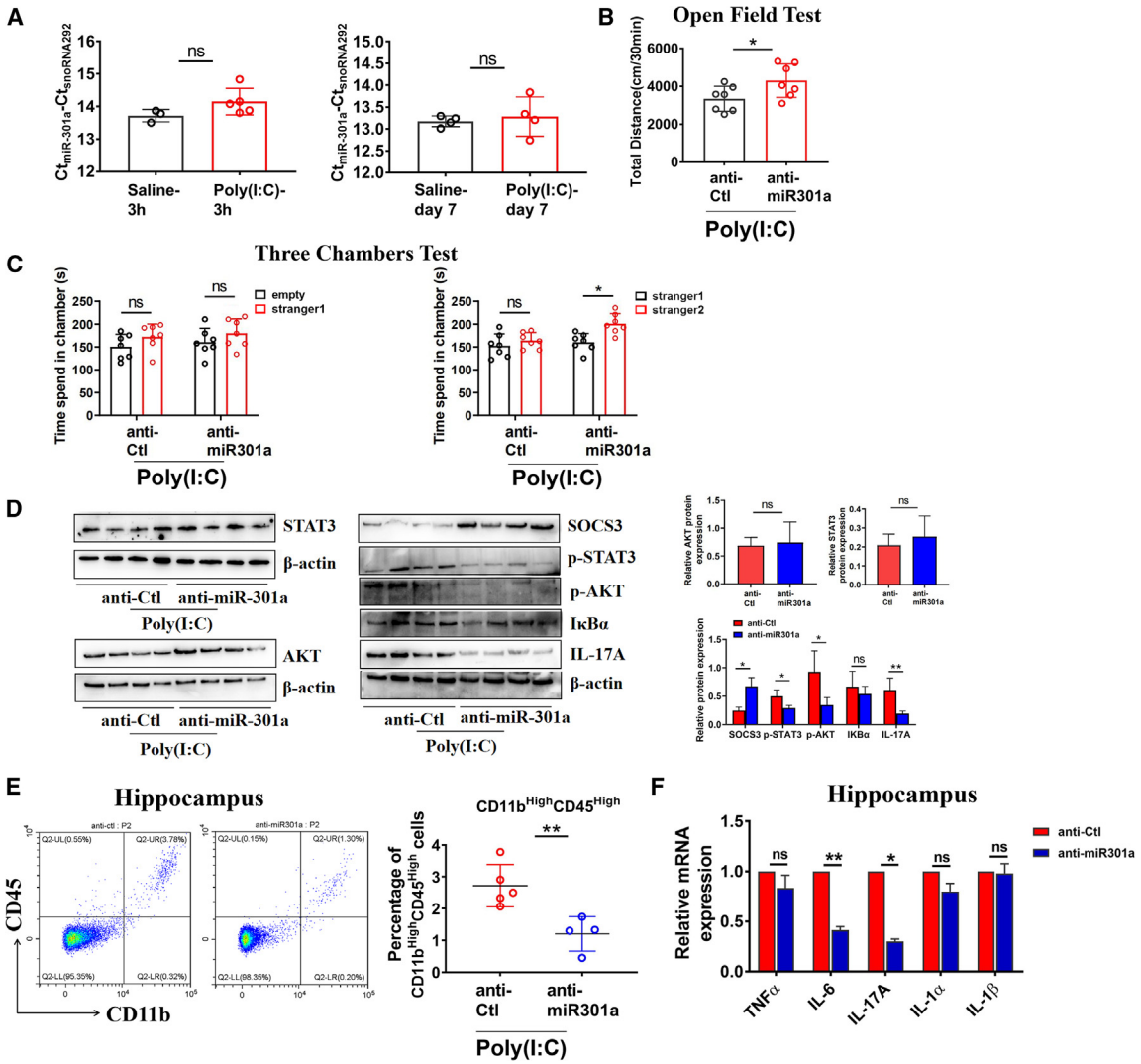

Figure 5. Knockdown of miR-301a reverse poly(I:C)-induced ASD-like behavior

(A) The expression of miR-301a was evaluated by RT-PCR in hippocampus from offspring of mothers injected with saline or poly(I:C). Brain tissues were harvested at 3 h and 7 days after the injection (saline, n = 3 and poly(I:C), n = 5 mice). (B) Offspring of mothers that were intraperitoneally injected with poly(I:C) plus anti-miR301a inhibitor (poly(I:C) + anti-miR-301a, n = 7) displayed less frequency, duration, and distance moved in the center in the open field compared with the offspring of mothers injected with poly(I:C) plus anti-Ctl (poly(I:C) + anti-Ctl, n = 7). (C) poly(I:C) + anti-miR-301a and poly(I:C) + anti-Ctl both showed no significant preference for stranger mice over objects, but poly(I:C) + anti-miR-301a showed significant preference to novel mice over familiar mice (n = 7). (D) The activation of STAT3 and AKT, and the expression of SOCS3 and IL-17A were measured and quantified by western blot in hippocampus from offspring with poly(I:C) + anti-miR-301a (n = 4) and poly(I:C) + anti-Ctl (n = 4). (E) Percentages of $CD11b^{high}$ $CD45^{high}$ cells isolated from hippocampus of offspring with poly(I:C) + anti-miR-301a (n = 4) and poly(I:C) + anti-Ctl (n = 5). (F) Cytokine expression was measured by RT-PCR in hippocampus tissues isolated from offspring with poly(I:C) + anti-miR-301a (n = 4) and poly(I:C) + anti-Ctl (n = 4). Each dot symbol represents an individual mouse. **p < 0.01 or *p < 0.05 indicates a significant difference between the indicated groups (two-tailed, unpaired Student's t test in A, B, D, E, and F, and two-way analysis of variance [ANOVA] in C). ns, not significant.

largely unchanged in poly(I:C)-induced ASDs (Figure 5A). Next, we employed this model to test whether the anti-miR-301a had a protective role in the poly(I:C)-induced ASDs. In a prevention study, we delivered anti-miR-301a oligonucleotide simultaneously with poly(I:C) into 12.5-day-old pregnant WT mice. Compared with the anti-miRNA control, the anti-miR-301a administration significantly reduced the partial ASD-like behaviors including social novelty and anxiety (Figures 5B and 5C). Consistent with the above results, the SOCS3 expression level was dramatically elevated, and the activation of STAT3 was significantly lower in the anti-miR-301a treatment than in the anti-miR control (Figure 5D). In addition, Phosphor-Akt and IL-17A were remarkably lower in the anti-miR-301a mice than anti-Ctl mice. However, the expression of IKBα remained unchanged. Furthermore, we evaluated the activation of the microglia

and several cytokines in the anti-miR-301a and poly(I:C)-treated pregnant mice. The number of microglia, evaluated by both CD45 and CD11b positive cells, was significantly reduced in hippocampus (Figure 5E) but not in cortex (Figures S10A and S10B). Two critical maternal cytokines, IL-6 and IL-17A, were constitutively decreased in the anti-miR-301a and poly(I:C)-treated offspring mice compared with the anti-miR control and poly(I:C) treatment (Figure 5F). These observations confirmed our hypothesis that miR-301a inhibition in mice embryo protected the poly(I:C)-induced ASD-like behaviors, which were highly correlated with the active state of STAT3 or AKT in hippocampus tissues.

DISCUSSION

miRNA dysfunctions have been recognized as pathology with a strong epidemiological association with ASD,[42] but the relationship has not been completely elucidated. In the present study, we revealed the effects of miR-301a deletion or knockdown on a variety of mouse behavioral phenotypes. We proved that miR-301a-deficient mice led to social disability, enhanced anxiety, and cognitive impairment, but miR-301a knockdown mice significantly improved social interactions and anxiety behavior in poly(I:C)-induced ASD mice, dependent on SOCS3/STAT3 and its downstream cytokines, IL-6 and IL-17A. These studies infer the complexity of miR-301a regulation in ASD under the two different conditions, constitutive knockout of miR-301a and short-term depletion of miR-301a in mice.

Increasing evidence demonstrates the aberrant expression of miR-130/301a in neurodevelopmental disorders and indicates the important posttranscriptional regulators of this family member in mental illness.[21,43] For example, miR-301a significantly downregulated in peripheral blood from ASD patients compared with healthy donors. miR-301a was also negatively correlated with seizure severity.[44] Moreover, overexpression of miR-301b significantly increased microglia activation and accelerated cognitive impairment.[20] In miR-103/301 family members, miR-301a was most highly expressed in brain tissues. Here, we observed that it significantly altered sociability and anxiety-like behavior in miR-301a deletion mice, although our previous study demonstrated that in *miR-301a*$^{-/-}$ mice there were no obvious developmental defects or physiological abnormalities.[29] We speculate that the differences in behavioral response between miR-301a deletion and inhibition in mice represented the diversity level of miR-301a and its targets in different brain regions. In addition, the miR-301a short-term inhibition did not lead to the same effects as in knockout of mice. Given that miR-301a exhibited more features in the immune system, future studies are needed to interrogate the involvement of miR-301a in psychopathology in mice with location-specific deletion.

In hippocampus RNA-sequencing, our results revealed that the transcriptional patterns in miR-301a deletion tissue did not change significantly, which confirmed the posttranscriptional role of miR-301a in brain tissues. Furthermore, the insulin secretion signaling pathway demonstrated a high activity status and enrichment in all three brain regions in *miR-301a*$^{-/-}$ mice compared with WT. Since insulin activates its intracellular effector, PI3K/AKT/mTOR that has been implicated in autism,[45] we hypothesize that hyperactivation of the insulin pathway found in *miR-301a*$^{-/-}$ mice might participate in the ASD-like behaviors. Furthermore, some unique signaling pathways were demonstrated in different brain regions, for example, some cytokine pathways in hippocampus, cholesterol biosynthesis in temporal cortex, and neuroinflammation signaling pathway in DRN. Together, these observations suggest that miR-301a contribution to the autism-like behavior alterations *in vivo* is dependent on the cellular context and specific regions.

We further identified three miR-301a predictable and potential targets, PDE10A, NCS1, and SCN1A, significant upregulation in N2A cells with knockdown of miR-301a. Other authors' results showed that the overexpression of PDE10A was previously identified to be related to the impairment of sociability and learning. Both NCS1[46] and SCN1A[39] have been linked to serious neuronal disorders. Interestingly, our results did not allow us to conclude whether an increase in the abundance of a specific mRNA represented the phenotype perturbation of miR-301a deficiency in mice, but rather implied that the individual miR-301a might regulate the expression of multiple mRNAs and happened to coincide with its distinct expression in multiple brain regions.

The specific target of miR-301a that we found was SOCS3, which inhibits cytokine signaling in numerous cell types, including immune cells and CNS. In CNS, the effects of SOCS3 expression are very different in that overexpression of SOCS3 in neurons decreases STAT3-mediated neurite outgrowth, whereas SOCS3 mediates the anti-inflammatory effects in microglia or astrocyte.[47,48] Our results from the *in vivo* study with the anti-miR-301a oligonucleotide showed that SOCS3 was significantly upregulated in miR-301a-restrained hippocampus, especially dominant in the microglia or astrocytes than in neurons. It was reported that the predominant function of SOCS3 was the inhibition of IL-6/STAT3 signaling.[49] Data show that it targets the JAK/STAT3 signaling pathways thus alleviating the symptoms of IL-6/MIA-associated autism.[3] We found that phosphorylated STAT3 and the expression of IL-6 and IL-17A were all significantly downregulated in mice after anti-miR-301a administration. This was for studying whether the down-regulation of miR-301a would benefit MIA-induced autism behaviors. As we expected, the social novelty and anxiety were improved in miR-301a-restrained mice, which was consistent with activation of SOCS3 and deactivation of STAT3. Unlike miR-301b, which activated NF-κB in depressive-like behavior, in our study, we found that the activation of AKT, but not the NF-κB, was significantly reduced in the hippocampus with anti-miR-301a inhibition, which further supported the diverse role of miR-130/301 associated with neurodevelopmental disorders. These findings suggested that miR-301a modulated the process of MIA during pregnancy and altered behavior of the offspring, through the negative regulation of SOCS3, and most probably many other targets. These results further demonstrated the key role of miR-301a in the complex network in autism.

Limitations of the study

Although our data support the idea that miR-301a is involved in neuropsychiatric disorders as a pro-inflammatory miRNA and could be a therapeutic target for preventing MIA-induced autism, our study has several limitations. First, anti-miR-301a inhibitor was intravenously administrated in mice. Inevitably, miR-301a inhibition influences the immune system in serum as well as the cells in mouse hippocampal tissue. Further study is needed to determine which type of hippocampus cells such as neurons or glia cells will suffer by miR-301a inhibitor administrated via brain stereotactic injection. Second, in our current study, we did not measure these behavioral phenotypes by using miR-301a conditional knockout mice. In future studies, it will be critical to determine the function of miR-301a in different cell types and regions of the brain and to establish how miR-301a deficiency will impair abnormal behaviors.

MATERIALS AND METHODS

Animal models and cell lines

Generation of *miR-301a*$^{-/-}$ mice in the C57BL/6 × 129S hybrid background has been described previously,[29] and all mouse experiments were performed under protocols approved by the Institutional Animal Care and Use Committee of South China Normal University and in accordance with the Guide for the Care and Use of Laboratory Animals. Three experimental mice models were used in our study: (1) MIA-induced mouse model of autism: pregnant mice were intraperitoneally injected with a 20 mg/kg single dose of poly(I:C) (Sigma) or saline on E12.5 d (embryonic day).[50] (2) knockdown of miR-301a *in vivo*: injection with a 20 mg/kg locked nucleic acid-modified oligonucleotide complementary to miR-301a (anti-miR-301a) or negative control (anti-Ctl) intravenously injected into 6-week-old WT mice.[20,51] (3) The inhibition of miR-301a in the MIA-induced mouse model of autism: pregnant mice were intraperitoneally injected with 20 mg/kg poly(I:C) plus 20 mg/kg of anti-miR-301a or anti-Ctl on E12.5d. N2A, SH-SY5Y, and HEK293T cells were cultured in DMEM supplemented with 10% fetal bovine serum and incubated at 37°C with 5% CO_2.

Behavior analysis

WT and *miR-301a*$^{-/-}$ mice (male, 20–25 g, age 6–8 weeks) were used for behavior analysis, including grooming test, marble buried test,[52] open field test,[53] three-chamber test,[54] and elevated plus maze.[55] GraphPad Prism software version 7.0 was employed to evaluate all comparisons. These behavior tests are described in detail in the following, and all test mice were transported to the experimental room for 30 min to habituate.

Grooming test

After adaptation, mice were placed in an empty 30 cm × 30 cm×40 cm transparent squirrel cage and allowed to explore for 10 min. The total time of grooming behavior of each mouse was recorded.

Marble buried test

After adaptation, mice were placed into the center of a transparent squirrel cage with a size of 30 cm × 30 cm × 40 cm with a height of 5 cm, and 20 black glass beads with a diameter of 14 mm were gently laid down on the surface of the cushion according to the sequence of 5 horizontal rows of 4 beads each. The number of buried glass beads was counted. The total recording time was 30 min.

Open field test

After adaptation, each mouse was placed separately in an empty 30 cm × 40 cm × 40 cm transparent box center. Then, the activity of mice was automatically recorded by a VersaMax animal behavior monitor. Each mouse was recorded for 30 min, and the residence time in the center of the box was recorded for the first 5 min to evaluate the anxiety level of the mice. The total 30-min exercise distance of mice was recorded to evaluate the exercise ability of mice.

Three-chamber test

After adaptation, test mice were placed in the central chamber of the equipment, and allowed to freely explore the equipment with a stranger mouse (male, 6-8 weeks of age, strange 1) under one cup in one of the side chambers for 10 min. Then another novel mouse (male, 6-8 weeks of age, strange 2) was placed under the cup in the opposite side chamber. The test mice were allowed to explore all chambers for 10 min and tracked using video to record the time spent around each target.

Elevated plus maze

The elevated plus maze has a pair of open arms and a pair of closed arms. Test mice were placed into the maze from the central grid to the closed arm. The time spent in closing and opening the arms of mice was recorded using Noduls software, so as to analyze the anxiety and fear state of mice.

Quantitative proteomic analysis

Differential expressed proteins in hippocampus, temporal cortex, and DRN from WT and *miR-301a*$^{-/-}$ mice were identified by using label-free quantitative proteomics.[56] Label-free quantitative MS proteomics identified differential protein expression has been described previously.[56] In our study, three brain regions, hippocampus, temporal cortex, and DRN, were used to analyze. First, samples were suspended in 8M urea lysis buffer, incubated at 4°C for 20 min, and further treated by ultra-sonication. The supernatant was collected after centrifugation at 14,000 × *g* for 20 min at 4°C. Based on the BCA assay, 200-μg aliquots were removed from each sample for further analysis. The supernatant was then incubated with dithiothreitol (5 mM) at room temperature for 1 h, followed by alkylation with iodoacetamide (10 mM) in the dark for 45 min. The final concentration of urea was then adjusted to 1 M via ultrafiltration to exclude the influence of high-concentration urea on follow-up experiments. Then, 4 μg of sequencing grade trypsin was added to the proteins for overnight incubation at 37°C after the proteins were resuspended in NH4HCO3 (50 mM), and the reaction was finally terminated by trifluoroacetic acid (0.4%). The proteins were desalted in 10 μg C18 columns and dried in a vacuum centrifuge. Then, 0.5 μg of the peptide mixture suspended in 0.1% formic acid was loaded onto a 2-cm self-packed trap column and then separated on a 75-μm inner

diameter column with a length of 12 cm over a 60-min gradient at a flow rate of 350 Nl/min. The separation was performed on a capillary reverse-phase column connected to a nanoflow high-performance liquid chromatograph instrument (Easy nLC1000 System) coupled to a Q Exactive HF mass spectrometer (Thermo Fisher). Raw MS data were processed using the MaxQuant software version 1.6.3.4.[57] Differential expressed proteins were identified by p value cutoff of 0.05 and the fold change was set at 1.5.

RNA-seq and DEG identification

Differentially expressed genes (DEGs) in hippocampus from WT and *miR-301a*$^{-/-}$ mice were identified by RNA-sequencing. Hippocampus mRNA profiles from WT and *miR-301a*$^{-/-}$ mice were generated with the NovaSeq6000 sequencing platform (Illumina, USA). Sequenced reads were mapped to the mm10 whole genome using Hisat2 v2.1.0 with default parameters and then calculated by HTSeq software.[58] The relative transcript abundance was measured in reads per kilobase of exon per million mapped reads (RPKM). DEGs were identified by an unpaired Student's t test with a p value cutoff of 0.05 and a fold change of more than 2.0 or less than 0.5.

Bioinformatics analysis

The online Tissue Atlas database was used to evaluate the distribution of miR-301a expression.[59] IPA was used to analyze canonical pathways and upstream regulator enrichment.[35] Protein-protein interaction analysis was applied to construct the protein interaction network by STRING v11.5 and Cytoscape v3.3.0.[60,61] Gene ontology and enriched pathways were analyzed by ToppGene prioritization.

Luciferase reporter assay

The 3′UTR sequence of SOCS3 was constructed into the plasmid, psiCHECK2 (C8021, Promega, USA). HEK293T cells were transfected with psiCHECK2-SOCS3-3′UTR and pre-miR-Ctl (control) or pre-miR-301a. After 48 h transfection, cells were lysed and the activities of luciferases were measured using the Dual-Luciferase Reporter Assay System (GeneCopoeia, USA) according to the manufacturer's protocol. Normalized data were calculated as the ratio of Renilla/Firefly luciferase activities.

Cell transfection

N2A and SH-SY5Y cells were transfected with LNA-anti-Control or LNA-Anti-miR-301a (Exiqon, Qiagen) using Lipofectamine RNAiMAX reagent (Thermo Fisher). After 48 h, the cells were collected for western blot.

RNA extraction and RT-PCR

RNA was reversely transcribed into cDNA with a Bio-Rad iScipt cDNA Synthesis Kit. The quality of RNA was determined by a Nano-drop spectrophotometer. RT-PCR was performed using the SYBR Green Supermix (Bio-Rad) and the primer sequences are shown in Table S5. RT-PCR for miR-301a detection was performed using the TaqMan assay (Thermo Fisher) with SNO292 as a reference and a CFX96 RT-PCR detection system (Bio-Rad, USA).

Western blot analysis

Proteins were extracted with RIPA buffer supplemented with a protease inhibitor. The samples were boiled for 5 min at 95°C. Equal amounts of protein were subjected to SDS-PAGE before being transferred to the polyvinylidene difluoride membrane. The membrane was blocked with 5% nonfat dry milk in Tris-buffered saline with 0.1% Tween 20 for 1 h and incubated with a primary antibody at 4°C overnight. The primary antibodies: IKBα (4814), SOCS3 (A0694), phospho-STAT3 (9145), total STAT3 (9139), phosphor-AKT (4060), total AKT (44D4) were purchased from CST, IL-17A (A12454), NCS1 (A13586), PDE10A (18078-1-AP), SCN1A (A10703), and β-actin (AC026) were purchased from Abclonal. Horseradish peroxidase-conjugated anti-rabbit or anti-mouse IgG was used as a secondary antibody. Immunoreactive proteins were visualized with a West Dura/Femto Chemiluminescent Kit (Thermo Fisher).

Immunofluorescence

The brain tissues were fixed in 10% formalin solution. Paraffin was used to encapsulate the chips, and then 3-μm-thick slices were prepared. The antigen was repaired with sodium citrate buffer in a water bath at 96°C. After washing with PBS and 3% H_2O_2 for 5 min, the sections were blocked with 10% normal goat serum. To measure the levels of SOCS3 and NeuN, tissue sections were incubated with these primary antibodies at 4°C overnight. After being rinsed with PBS, the sections were incubated with goat polyclonal secondary antibody to rabbit IgG (Alexa Fluor 488, Invitrogen, ab150077) or goat polyclonal secondary antibody to mouse IgG (Alexa Fluor 594, Invitrogen, ab150116) for 2 h at room temperature. After PBS rinse, the sections were incubated with 1 μg/mL DAPI (Sigma) for 10 min, and images were acquired using Olympus IX51 fluorescence microscope and cellSens software.

Flow cytometry

Hippocampus and cortex of 6-week-old WT and *miR-301a*$^{-/-}$ mice were dissected. Tissues were dissected and were incubated with 0.25% trypsin to digest for 15–30 min in a 37°C water bath. After digestion, tissues were washed twice with PBS and strainer mesh was used to obtain single cells. The single-cell suspensions were stained with anti-CD11b-FITC (BD, USA) and anti-CD45-PE (BD, USA) at 4°C for 30 min. All events were acquired using CytoFLEX (Beckman Coulter) equipment according to standard procedures.

Statistical analyses

All data are presented as the means ± standard deviation (SD). All statistical analysis was performed using the SPSS16.0 software (SPSS Inc., Chicago). An unpaired two-tailed Student's t test was performed for two-group comparisons, two-way analysis of variance (ANOVA) was performed for multiple factors, and one-way ANOVA was performed for multiple group comparisons. Statistical significance was set for p values * <0.05 or ** <0.01.

DATA AND CODE AVAILABILITY

The data that support the findings of this study were submitted to the Gene Expression Omnibus Database (Accession: GSE194389). The

data are available from https://www.ncbi.nlm.nih.gov/geo/query/acc.cgi?acc=GSE194389.

SUPPLEMENTAL INFORMATION

Supplemental information can be found online at https://doi.org/10.1016/j.omtn.2024.102136.

ACKNOWLEDGMENTS

This study was supported by grants from the Key Area Research and Development Program of Guangdong Province (2019B030335001, 2018B030335001), the National Natural Science Foundation of China (82072697, 31771127), and National Social Science Foundation of China (20&ZD296).

AUTHOR CONTRIBUTIONS

X.L., Q.F., and M.Z. performed most of the experiments. Z.Z. and M.W. did the behavioral experiments. Y.L., Y.H., F.Z., and K.C. participated in data analysis and animal experiments. R.C. and X.M. designed and wrote the manuscript. All authors reviewed the manuscript and approved the submission.

DECLARATION OF INTERESTS

The authors declare no competing interests.

REFERENCES

1. King, B.H., Navot, N., Bernier, R., and Webb, S.J. (2014). Update on diagnostic classification in autism. Curr. Opin. Psychiatr. *27*, 105–109.
2. Nadeem, M.S., Hosawi, S., Alshehri, S., Ghoneim, M.M., Imam, S.S., Murtaza, B.N., and Kazmi, I. (2021). Symptomatic, Genetic, and Mechanistic Overlaps between Autism and Alzheimer's Disease. Biomolecules *11*.
3. Estes, M.L., and McAllister, A.K. (2016). Maternal immune activation: Implications for neuropsychiatric disorders. Science *353*, 772–777.
4. Ye, J., Wang, H., Cui, L., Chu, S., and Chen, N. (2021). The progress of chemokines and chemokine receptors in autism spectrum disorders. Brain Res. Bull. *174*, 268–280.
5. Mouihate, A., and Mehdawi, H. (2016). Toll-like receptor 4-mediated immune stress in pregnant rats activates STAT3 in the fetal brain: role of interleukin-6. Pediatr. Res. *79*, 781–787.
6. Kwon, S.H., Han, J.K., Choi, M., Kwon, Y.J., Kim, S.J., Yi, E.H., Shin, J.C., Cho, I.H., Kim, B.H., Jeong Kim, S., et al. (2017). Dysfunction of Microglial STAT3 Alleviates Depressive Behavior via Neuron-Microglia Interactions. Neuropsychopharmacology : official publication of the American College of Neuropsychopharmacology *42*, 2072–2086.
7. Ahmad, S.F., Ansari, M.A., Nadeem, A., Bakheet, S.A., Alsanea, S., Al-Hosaini, K.A., Mahmood, H.M., Alzahrani, M.Z., and Attia, S.M. (2020). Inhibition of tyrosine kinase signaling by tyrphostin AG126 downregulates the IL-21/IL-21R and JAK/STAT pathway in the BTBR mouse model of autism. Neurotoxicology *77*, 1–11.
8. Ahmad, S.F., Ansari, M.A., Nadeem, A., Bakheet, S.A., Alanazi, A.Z., Alsanea, S., As Sobeai, H.M., Almutairi, M.M., Mahmood, H.M., and Attia, S.M. (2019). The Stat3 inhibitor, S3I-201, downregulates lymphocyte activation markers, chemokine receptors, and inflammatory cytokines in the BTBR T(+) Itpr3(tf)/J mouse model of autism. Brain Res. Bull. *152*, 27–34.
9. Ahmad, S.F., Ansari, M.A., Nadeem, A., Bakheet, S.A., Alshammari, M.A., Khan, M.R., Alsaad, A.M.S., and Attia, S.M. (2018). S3I-201, a selective Stat3 inhibitor, restores neuroimmune function through upregulation of Treg signaling in autistic BTBR T(+) Itpr3(tf)/J mice. Cell. Signal. *52*, 127–136.
10. Reisinger, S.N., Sideromenos, S., Horvath, O., Derdak, S., Cicvaric, A., Monje, F.J., Bilban, M., Häring, M., Glat, M., and Pollak, D.D. (2021). STAT3 in the dorsal raphe gates behavioural reactivity and regulates gene networks associated with psychopathology. Mol. Psychiatr. *26*, 2886–2899.
11. Meyer, U. (2014). Prenatal poly(i:C) exposure and other developmental immune activation models in rodent systems. Biol. Psychiatr. *75*, 307–315.
12. Choi, G.B., Yim, Y.S., Wong, H., Kim, S., Kim, H., Kim, S.V., Hoeffer, C.A., Littman, D.R., and Huh, J.R. (2016). The maternal interleukin-17a pathway in mice promotes autism-like phenotypes in offspring. Science *351*, 933–939.
13. Ponzio, N.M., Servatius, R., Beck, K., Marzouk, A., and Kreider, T. (2007). Cytokine levels during pregnancy influence immunological profiles and neurobehavioral patterns of the offspring. Ann. N. Y. Acad. Sci. *1107*, 118–128.
14. Kummer, K.K., Zeidler, M., Kalpachidou, T., and Kress, M. (2021). Role of IL-6 in the regulation of neuronal development, survival and function. Cytokine *144*, 155582.
15. Reed, M.D., Yim, Y.S., Wimmer, R.D., Kim, H., Ryu, C., Welch, G.M., Andina, M., King, H.O., Waisman, A., Halassa, M.M., et al. (2020). IL-17a promotes sociability in mouse models of neurodevelopmental disorders. Nature *577*, 249–253.
16. Cheng, Y., Wang, Z.M., Tan, W., Wang, X., Li, Y., Bai, B., Li, Y., Zhang, S.F., Yan, H.L., Chen, Z.L., et al. (2018). Partial loss of psychiatric risk gene Mir137 in mice causes repetitive behavior and impairs sociability and learning via increased Pde10a. Nat. Neurosci. *21*, 1689–1703.
17. Lou, D., Wang, J., and Wang, X. (2019). miR-124 ameliorates depressive-like behavior by targeting STAT3 to regulate microglial activation. Mol. Cell. Probes *48*, 101470.
18. Hicks, S.D., and Middleton, F.A. (2016). A Comparative Review of microRNA Expression Patterns in Autism Spectrum Disorder. Front. Psychiatr. *7*, 176.
19. Wang, J., and Zhao, J. (2021). MicroRNA Dysregulation in Epilepsy: From Pathogenetic Involvement to Diagnostic Biomarker and Therapeutic Agent Development. Front. Mol. Neurosci. *14*, 650372.
20. Tang, C.Z., Zhang, D.F., Yang, J.T., Liu, Q.H., Wang, Y.R., and Wang, W.S. (2019). Overexpression of microRNA-301b accelerates hippocampal microglia activation and cognitive impairment in mice with depressive-like behavior through the NF-kappaB signaling pathway. Cell Death Dis. *10*, 316.
21. Alural, B., Genc, S., and Haggarty, S.J. (2017). Diagnostic and therapeutic potential of microRNAs in neuropsychiatric disorders: Past, present, and future. Prog. Neuro-Psychopharmacol. Biol. Psychiatry *73*, 87–103.
22. Alacam, H., Akgun, S., Akca, H., Ozturk, O., Kabukcu, B.B., and Herken, H. (2016). miR-181b-5p, miR-195-5p and miR-301a-3p are related with treatment resistance in schizophrenia. Psychiatr. Res. *245*, 200–206.
23. Zhang, Y., Chen, M., Qiu, Z., Hu, K., McGee, W., Chen, X., Liu, J., Zhu, L., and Wu, J.Y. (2016). MiR-130a regulates neurite outgrowth and dendritic spine density by targeting MeCP2. Protein Cell *7*, 489–500.
24. Ma, X., Kumar, M., Choudhury, S.N., Becker Buscaglia, L.E., Barker, J.R., Kanakamedala, K., Liu, M.F., and Li, Y. (2011). Loss of the miR-21 allele elevates the expression of its target genes and reduces tumorigenesis. Proc. Natl. Acad. Sci. USA *108*, 10144–10149.
25. Wang, J., Li, X., Zhong, M., Wang, Y., Zou, L., Wang, M., Gong, X., Wang, X., Zhou, C., Ma, X., and Liu, M. (2020). miR-301a Suppression within Fibroblasts Limits the Progression of Fibrosis through the TSC1/mTOR Pathway. Mol. Ther. Nucleic Acids *21*, 217–228.
26. Tsai, P.T., Hull, C., Chu, Y., Greene-Colozzi, E., Sadowski, A.R., Leech, J.M., Steinberg, J., Crawley, J.N., Regehr, W.G., and Sahin, M. (2012). Autistic-like behaviour and cerebellar dysfunction in Purkinje cell Tsc1 mutant mice. Nature *488*, 647–651.
27. Getz, S.A., Tariq, K., Marchand, D.H., Dickson, C.R., Howe Vi, J.R., Skelton, P.D., Wang, W., Li, M., Barry, J.M., Hong, J., and Luikart, B.W. (2022). PTEN Regulates Dendritic Arborization by Decreasing Microtubule Polymerization Rate. J. Neurosci. *42*, 1945–1957.
28. Mycko, M.P., Cichalewska, M., Machlanska, A., Cwiklinska, H., Mariasiewicz, M., and Selmaj, K.W. (2012). MicroRNA-301a regulation of a T-helper 17 immune response controls autoimmune demyelination. Proc. Natl. Acad. Sci. USA *109*, E1248–E1257.
29. Ma, X., Yan, F., Deng, Q., Li, F., Lu, Z., Liu, M., Wang, L., Conklin, D.J., McCracken, J., Srivastava, S., et al. (2015). Modulation of tumorigenesis by the pro-inflammatory

microRNA miR-301a in mouse models of lung cancer and colorectal cancer. Cell Discov. *1*, 15005.

30. Ji-Xu, A., and Vincent, A. (2020). Maternal Immunity in Autism Spectrum Disorders: Questions of Causality, Validity, and Specificity. J. Clin. Med. *9*, 2590.
31. Nakata, M., Kimura, R., Funabiki, Y., Awaya, T., Murai, T., and Hagiwara, M. (2019). MicroRNA profiling in adults with high-functioning autism spectrum disorder. Mol. Brain *12*, 82.
32. Ginsberg, M.R., Rubin, R.A., Falcone, T., Ting, A.H., and Natowicz, M.R. (2012). Brain transcriptional and epigenetic associations with autism. PLoS One *7*, e44736.
33. Hwang, Y.I.J., Arnold, S., Srasuebkul, P., and Trollor, J. (2020). Understanding anxiety in adults on the autism spectrum: An investigation of its relationship with intolerance of uncertainty, sensory sensitivities and repetitive behaviours. Autism *24*, 411–422.
34. Gandal, M.J., Zhang, P., Hadjimichael, E., Walker, R.L., Chen, C., Liu, S., Won, H., van Bakel, H., Varghese, M., Wang, Y., et al. (2018). Transcriptome-wide isoform-level dysregulation in ASD, schizophrenia, and bipolar disorder. Science *362*, eaat8127.
35. Li, X., Zhong, M., Wang, J., Wang, L., Lin, Z., Cao, Z., Huang, Z., Zhang, F., Li, Y., Liu, M., and Ma, X. (2019). miR-301a promotes lung tumorigenesis by suppressing Runx3. Mol. Cancer *18*, 99.
36. Handley, M.T.W., Lian, L.Y., Haynes, L.P., and Burgoyne, R.D. (2010). Structural and functional deficits in a neuronal calcium sensor-1 mutant identified in a case of autistic spectrum disorder. PLoS One *5*, e10534.
37. Talkowski, M.E., Rosenfeld, J.A., Blumenthal, I., Pillalamarri, V., Chiang, C., Heilbut, A., Ernst, C., Hanscom, C., Rossin, E., Lindgren, A.M., et al. (2012). Sequencing chromosomal abnormalities reveals neurodevelopmental loci that confer risk across diagnostic boundaries. Cell *149*, 525–537.
38. Papp-Hertelendi, R., Tényi, T., Hadzsiev, K., Hau, L., Benyus, Z., and Csábi, G. (2018). First report on the association of SCN1A mutation, childhood schizophrenia and autism spectrum disorder without epilepsy. Psychiatr. Res. *270*, 1175–1176.
39. Han, S., Tai, C., Westenbroek, R.E., Yu, F.H., Cheah, C.S., Potter, G.B., Rubenstein, J.L., Scheuer, T., de la Iglesia, H.O., and Catterall, W.A. (2012). Autistic-like behaviour in Scn1a+/- mice and rescue by enhanced GABA-mediated neurotransmission. Nature *489*, 385–390.
40. Huang, J., Xu, X., and Yang, J. (2021). miRNAs Alter T Helper 17 Cell Fate in the Pathogenesis of Autoimmune Diseases. Front. Immunol. *12*, 593473.
41. Cianciulli, A., Calvello, R., Porro, C., Trotta, T., and Panaro, M.A. (2017). Understanding the role of SOCS signaling in neurodegenerative diseases: Current and emerging concepts. Cytokine Growth Factor Rev. *37*, 67–79.
42. Wu, Y.E., Parikshak, N.N., Belgard, T.G., and Geschwind, D.H. (2016). Genome-wide, integrative analysis implicates microRNA dysregulation in autism spectrum disorder. Nat. Neurosci. *19*, 1463–1476.
43. van den Berg, M.M.J., Krauskopf, J., Ramaekers, J.G., Kleinjans, J.C.S., Prickaerts, J., and Briedé, J.J. (2020). Circulating microRNAs as potential biomarkers for psychiatric and neurodegenerative disorders. Prog. Neurobiol. *185*, 101732.
44. Wang, J., Tan, L., Tan, L., Tian, Y., Ma, J., Tan, C.C., Wang, H.F., Liu, Y., Tan, M.S., Jiang, T., and Yu, J.T. (2015). Circulating microRNAs are promising novel biomarkers for drug-resistant epilepsy. Sci. Rep. *5*, 10201.
45. Stern, M. (2011). Insulin signaling and autism. Front. Endocrinol. *2*, 54.
46. Fischer, T.T., Nguyen, L.D., and Ehrlich, B.E. (2021). Neuronal calcium sensor 1 (NCS1) dependent modulation of neuronal morphology and development. Faseb. J. *35*, e21873.
47. Baker, B.J., Akhtar, L.N., and Benveniste, E.N. (2009). SOCS1 and SOCS3 in the control of CNS immunity. Trends Immunol. *30*, 392–400.
48. Zhang, L., Lu, X., Gong, L., Cui, L., Zhang, H., Zhao, W., Jiang, P., Hou, G., and Hou, Y. (2021). Tetramethylpyrazine Protects Blood-Spinal Cord Barrier Integrity by Modulating Microglia Polarization Through Activation of STAT3/SOCS3 and Inhibition of NF-small ka, CyrillicB Signaling Pathways in Experimental Autoimmune Encephalomyelitis Mice. Cell. Mol. Neurobiol. *41*, 717–731.
49. Xue, Y., Zhou, Y., Bao, W., Fu, Q., Hao, H., Han, L., Zhang, X., Tian, X., and Zhang, M. (2021). STAT3 and IL-6 Contribute to Corticosteroid Resistance in an OVA and Ozone-induced Asthma Model with Neutrophil Infiltration. Front. Mol. Biosci. *8*, 717962.
50. Naviaux, R.K., Zolkipli, Z., Wang, L., Nakayama, T., Naviaux, J.C., Le, T.P., Schuchbauer, M.A., Rogac, M., Tang, Q., Dugan, L.L., and Powell, S.B. (2013). Antipurinergic therapy corrects the autism-like features in the poly(IC) mouse model. PLoS One *8*, e57380.
51. Ma, X., Conklin, D.J., Li, F., Dai, Z., Hua, X., Li, Y., Xu-Monette, Z.Y., Young, K.H., Xiong, W., Wysoczynski, M., et al. (2015). The oncogenic microRNA miR-21 promotes regulated necrosis in mice. Nat. Commun. *6*, 7151.
52. Silverman, J.L., Yang, M., Lord, C., and Crawley, J.N. (2010). Behavioural phenotyping assays for mouse models of autism. Nat. Rev. Neurosci. *11*, 490–502.
53. Kraeuter, A.K., Guest, P.C., and Sarnyai, Z. (2019). The Open Field Test for Measuring Locomotor Activity and Anxiety-Like Behavior. Methods Mol. Biol. *1916*, 99–103.
54. Yang, M., Silverman, J.L., and Crawley, J.N. (2011). Automated three-chambered social approach task for mice. Curr. Protoc. Neurosci. *56*. Unit 8 26.
55. Walf, A.A., and Frye, C.A. (2007). The use of the elevated plus maze as an assay of anxiety-related behavior in rodents. Nat. Protoc. *2*, 322–328.
56. Leitner, D.F., Mills, J.D., Pires, G., Faustin, A., Drummond, E., Kanshin, E., Nayak, S., Askenazi, M., Verducci, C., Chen, B.J., et al. (2021). Proteomics and Transcriptomics of the Hippocampus and Cortex in SUDEP and High-Risk SUDEP Patients. Neurology *96*, e2639–e2652.
57. Cox, J., and Mann, M. (2008). MaxQuant enables high peptide identification rates, individualized p.p.b.-range mass accuracies and proteome-wide protein quantification. Nat. Biotechnol. *26*, 1367–1372.
58. Kim, D., Langmead, B., and Salzberg, S.L. (2015). HISAT: a fast spliced aligner with low memory requirements. Nat. Methods *12*, 357–360.
59. Ludwig, N., Leidinger, P., Becker, K., Backes, C., Fehlmann, T., Pallasch, C., Rheinheimer, S., Meder, B., Stähler, C., Meese, E., and Keller, A. (2016). Distribution of miRNA expression across human tissues. Nucleic Acids Res. *44*, 3865–3877.
60. Szklarczyk, D., Morris, J.H., Cook, H., Kuhn, M., Wyder, S., Simonovic, M., Santos, A., Doncheva, N.T., Roth, A., Bork, P., et al. (2017). The STRING database in 2017: quality-controlled protein-protein association networks, made broadly accessible. Nucleic Acids Res. *45*, D362–D368.
61. Shannon, P., Markiel, A., Ozier, O., Baliga, N.S., Wang, J.T., Ramage, D., Amin, N., Schwikowski, B., and Ideker, T. (2003). Cytoscape: a software environment for integrated models of biomolecular interaction networks. Genome Res. *13*, 2498–2504.